Human iPSC-Derived Cardiomyocyte Disease Modeling of Friedreich's Ataxia and Duchenne Muscular Dystrophy for Therapeutic Assessment

Jessica Koepke, Mariana Argenziano, Shushant Jain
Ncardia Services BV, Leiden, The Netherlands, support@ncardia.com, www.ncardia.com

Background

The reprogramming of patient-derived fibroblasts into human induced pluripotent stem cells (hiPSCs) and their subsequent differentiation into cardiomyocytes (hiPSC-CMs) has enabled the development of physiologically relevant in vitro models for human cardiac diseases. Here, we present data from models of Friedreich's ataxia (FRDA) and Duchenne muscular dystrophy (DMD), demonstrating a drug-screening platform with closer fidelity to human pathophysiology. These models recapitulate key cellular disease phenotypes, offering advantages over murine and other animal models.

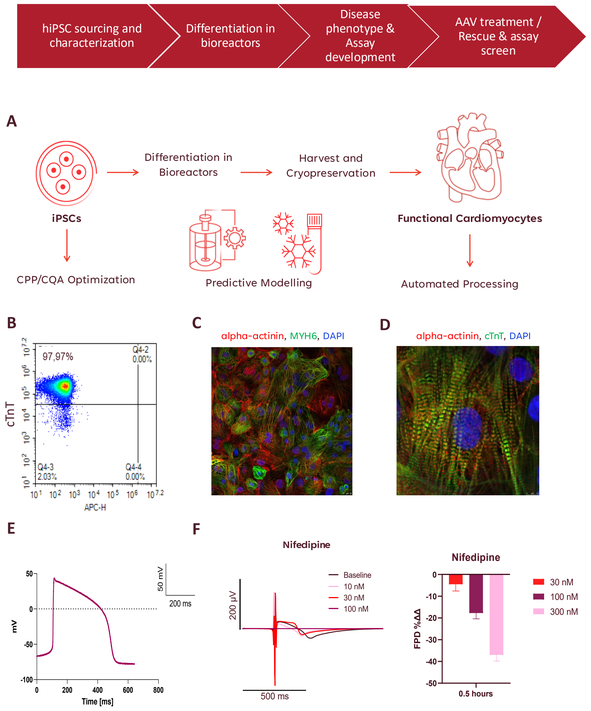

Figure 1 . Large scale differentiation and characterization of iPSC-CMs
(A) Ncardia's medium scale and large bioreactor systems can yield ~150 million to more than 10B of assay-ready cells.
(B) iPSC-CMs express ≥ 90% purity of cardiac TroponinT (cTnT) positive cells.
(C) ICC showing staining for cardiac markers alpha-actinin (red) and MYH6 (green). iPSC-CMs show aligned myofibrils and preserved sarcomere organization.
(D) ICC showing staining for cardiac markers alpha-actinin (red) and cTnT (green). iPSC-CMs show aligned myofibrils and preserved sarcomere organization.
(E) Action potential profile of iPSC derived Cardiomyocytes mirrors that of human ventricular cardiomyocytes.
(F) Respond to ion channel blockers such as nifedipine in a dose dependent manner.

1. iPSC-CMs from FRDA patients showed lower frataxin

As expected, FRDA patient-derived hiPSC-CMs exhibited significantly lower frataxin expression compared to controls. Calcium transients recorded via the FDSS/µCell kinetic reader (Hamamatsu) revealed prolonged calcium transient duration and decay in FRDA hiPSC-CMs.

Using flow cytometry with a CellROX probe, we detected a significant increase in ROS levels in FRDA hiPSC-CMs relative to controls. Additionally, both FRDA hiPSC-CMs exhibited aberrant calcium handling.

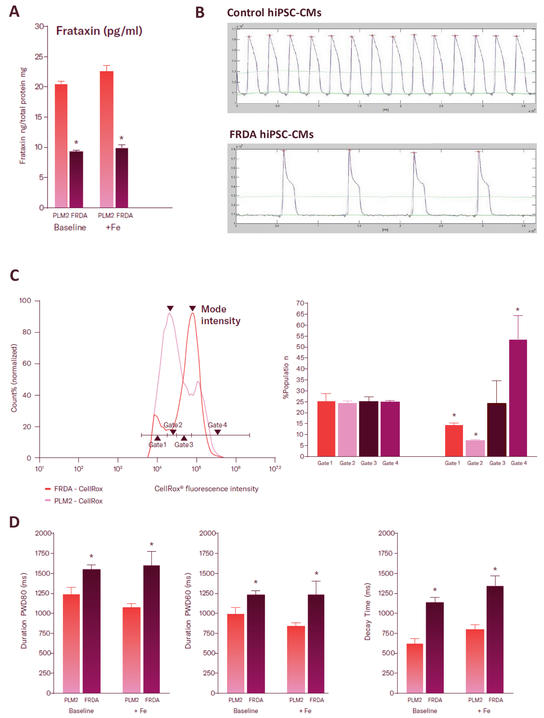

Figure 2. iPSC-CMs from the FRDA patient line showed significantly lower amounts of frataxin protein compared to a healthy control line
(A) normalized (frataxin protein ng per mg of total protein) frataxin levels under baseline and iron supplemented conditions (p <0.001, t-test, n = 3).
(B) Representative traces of Ca^{2+} transients of FRDA (upper) and control (lower) hiPSC-CMs.
(C) FACS histograms of both control and FRDA hiPSC-CMs and four-gate quantification approach was used for quantifying fluorescence intensity (FI) within CellRox positive populations of both samples (p <0.001, t-test, n = 6).
(D) Parameters of Ca^{2+} transient durations at 80% and 60% of signal decay (PWD80 and PWD60, respectively) as well as the Ca^{2+} transient decay extrapolated from recordings (p <0.001, t-test, n = 6).

2. iPSC-CMs from DMD patients showed no expression of dystrophin

DMD hiPSC-CMs showed an absence of endogenous dystrophin. Additionally, DMD hiPSC-CMs exhibited aberrant calcium handling. Impedance-based contractility measurements and calcium transient recordings showed significantly reduced calcium transient amplitude and duration compared to controls.

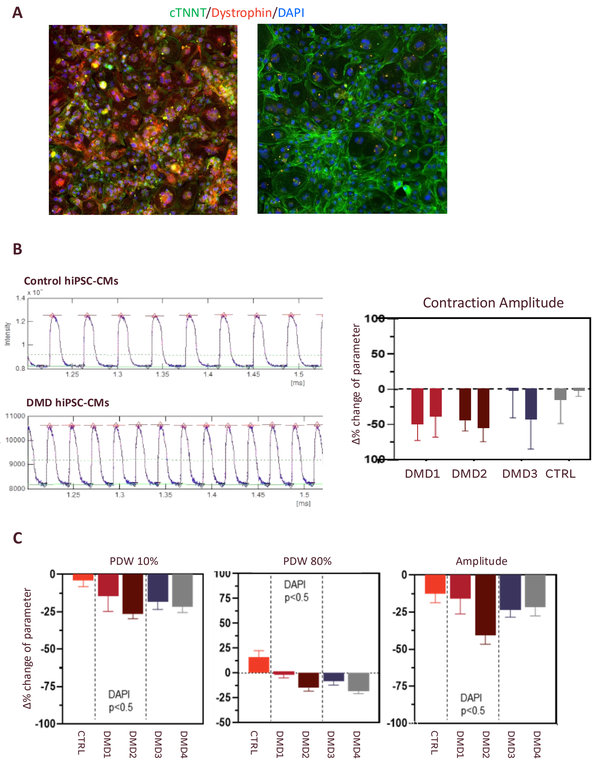

Figure 3. DMD iPSC derived cardiomyocytes showed no expression of endogenous dystrophin.
(A) Confirmed lack of endogenously expressed dystrophin in DMD iPSC-cardiomyocytes by ICC.
(B) Decreased contraction amplitude in three lines of DMD iPSC-cardiomyocytes. Δ% to mean of control iPSC-CMs amplitude.
(C) Representative traces of Ca^{2+} transients of DMD (upper) and control (lower) hiPSC-CMs.
(D) Parameters of Ca^{2+} transient durations at 10% and 80% of signal decay (PWD10 and PWD80, respectively) as well as the Ca^{2+} amplitude from recordings. Δ% Change to mean of control iPSC-CMs.

3. Functional Rescue of FRDA and DMD iPSC-CMs by AAV-Mediated Gene Therapy

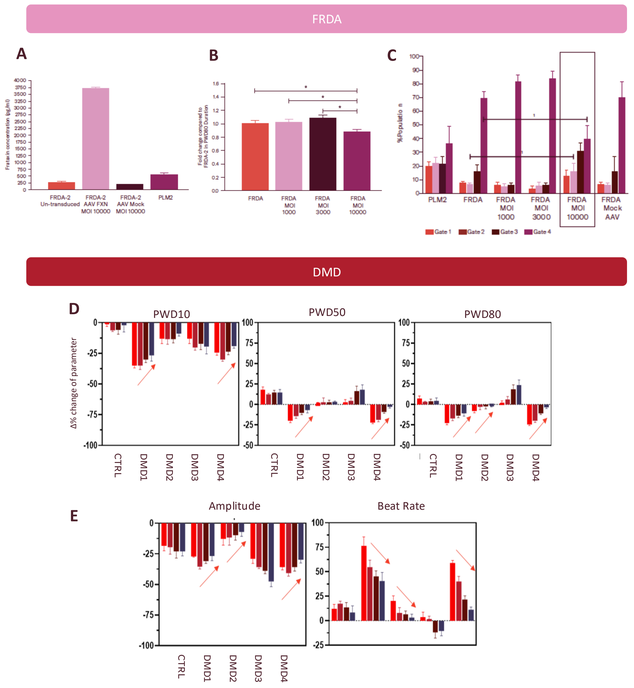

Figure 4. Characterization of FRDA and DMD iPSC-CMs and Rescue by AAV-Mediated Gene Therapy.
(A) Frataxin levels in control, FRDA and AAV-FXN transduced FRDA hiPSC-CMs (p <0.001, One Way ANOVA, Tukey test, n = 3). **(B)** Ca2+ transient duration in FRDA and AAV-FXN transduced FRDA hiPSC-CMs (p <0.05, One Way ANOVA, n = 6). **(C)** FACS quantification of fluorescence intensity for control, FRDA and AAV-FXN transduced FRDA hiPSC-CMs (p <0.05, One Way ANOVA, Tukey test, n = 3). **(D)** Parameters of Ca^{2+} transient durations at 10%, 50% and 80% of signal decay in AAV-Dystrophin transduced DMD iPSC-CMs compared to controls (PWD10, PDW50 and PWD80, respectively) as well. Δ% Change to mean of control iPSC-CMs. **(E)** Ca^{2+} amplitude and beat rate recordings in AAV-Dystrophin transduced DMD iPSC-CMs compared to controls . Δ% Change to mean of control iPSC-CMs.

Conclusions

By leveraging controlled stirred-tank bioreactors, we achieved high-yield, high-purity hiPSC-CM production suitable for large-scale screening of new therapeutics.

Our findings confirmed expected molecular deficiencies in FRDA and DMD models and corresponding disease-phenotypes.

These platforms were successfully used for therapeutic assessment and showed phenotype-rescue of key disease hallmarks through AAV-mediated gene delivery of Frataxin or Dystrophin.